Computational and Applied Mathematics (2020) 39:271
https://doi.org/10.1007/s40314-020-01322-4

Existence, uniqueness, and numerical solutions for two-dimensional nonlinear fractional Volterra and Fredholm integral equations in a Banach space

Khosrow Maleknejad[1] · **Jalil Rashidinia**[1] · **Tahereh Eftekhari**[1]

Received: 21 October 2019 / Revised: 2 August 2020 / Accepted: 1 September 2020 /
Published online: 12 September 2020

Abstract

The purpose of this research is to provide sufficient conditions for the local and global existence of solutions for two-dimensional nonlinear fractional Volterra and Fredholm integral equations, based on the Schauder's and Tychonoff's fixed-point theorems. Also, we provide sufficient conditions for the uniqueness of the solutions. Moreover, we use operational matrices of hybrid of two-dimensional block-pulse functions and two-variable shifted Legendre polynomials via collocation method to find approximate solutions of the mentioned equations. In addition, a discussion on error bound and convergence analysis of the proposed method is presented. Finally, the accuracy and efficiency of the presented method are confirmed by solving three illustrative examples and comparing the results of the proposed method with other existing numerical methods in the literature.

Keywords Two-dimensional nonlinear fractional Volterra and Fredholm integral equations · Existence and uniqueness · Banach space · Hybrid functions · Operational matrices · Collocation method · Convergence analysis

Mathematics Subject Classification 26A33 · 33C45 · 65N35

Communicated by José Tenreiro Machado.

✉ Khosrow Maleknejad
maleknejad@iust.ac.ir

Jalil Rashidinia
rashidinia@iust.ac.ir

Tahereh Eftekhari
t.eftekhari2009@gmail.com

[1] School of Mathematics, Iran University of Science and Technology (IUST), Narmak, Tehran 16846 13114, Iran

1 Introduction

The fractional calculus deals with derivatives and integrals to an arbitrary order. In recent years, a large number of scientific and engineering problems involving fractional calculus. It provides more accurate models of systems under consideration. The applications of fractional calculus have been demonstrated by many authors. Many systems in interdisciplinary fields, such as biological systems (Ahmed and Elgazzar 2007; Zalp and Demirci 2011), turbulence (Chen 2006), anomalous diffusion (Chen et al. 2010; Sun et al. 2009), viscoelastic systems (Rossikhin and Shitikova 1997), and partial bed-load transport (Sun et al. 2015), can be described with the help of fractional derivatives. Moreover, various problems in fluid mechanics, biology, physics, physiology, optics, and climatology can be modeled by fractional integral equations (Atanackovic and Stankovic 2004; Evans et al. 2017). In many situations, analytic solutions of fractional integral and differential equations are not available, or may these equations not be directly solvable. Therefore, finding efficient numerical methods to approximate the solutions of these equations has become the main objective of many mathematicians. For a review on numerical methods, see, for instance, (Amin et al. 2021; Aminikhah et al. 2017; Dahaghin and Hassani 2017; Esmaeili et al. 2011; Fathizadeh et al. 2017; Hassani et al. 2019; Hassani and Naraghirad 2019; Hesameddini and Shahbazi 2018; Hassani et al. 2019a, b; Jabari Sabeg et al. 2017; Kılıçman and Al Zhour 2007; Li and Shah 2017; Mohammadi Rick and Rashidinia 2019; Maleknejad et al. 2018, 2020a, b, c; Mashoof and Refahi Shekhani 2017; Mirzaee and Samadyar 2019; Najafalizadeh and Ezzati 2016; Nouri et al. 2018; Pourbabaee and Saadatmandi 2019; Permoon et al. 2016; Rahimkhani et al. 2018; Samadyar and Mirzaee 2019; Shah and Wang 2019; Zhu and Fan 2012).

In this research study, the following fractional integral equations of the second kind are considered:

Two-dimensional nonlinear fractional Volterra integral equations (2D-NFVIEs):

$$f(x,y)=g(x,y)+\frac{1}{\Gamma(\iota_1)\Gamma(\iota_2)}\int_0^x\int_0^y (x-\tau)^{\iota_1-1}(y-\varsigma)^{\iota_2-1}k(x,y,\tau,\varsigma,f(\tau,\varsigma))\mathrm{d}\varsigma\mathrm{d}\tau, \tag{1}$$

Two-dimensional nonlinear fractional Fredholm integral equations (2D-NFFIEs):

$$f(x,y)=g(x,y)+\frac{1}{\Gamma(\iota_1)\Gamma(\iota_2)}\int_0^{\ell_1}\int_0^{\ell_2} (\ell_1-\tau)^{\iota_1-1}(\ell_2-\varsigma)^{\iota_2-1}k(x,y,\tau,\varsigma,f(\tau,\varsigma))\mathrm{d}\varsigma\mathrm{d}\tau, \tag{2}$$

where $f(x,y)$, $k(x,y,\tau,\varsigma,f(\tau,\varsigma))$ are unknown functions and $g(x,y)$ is a given function. Also, $\iota_1,\ \iota_2>0$ and $(x,y)\in\Omega=[0,\ell_1]\times[0,\ell_2]$.

The outline of this paper is as follows. First, in Sect. 2, a review of two definitions required in this paper is given. In Sect. 3, sufficient conditions for the existence and uniqueness of solutions for 2D-NFVIEs and 2D-NFFIEs are provided. Also, in Sect. 4, the hybrid of two-dimensional block-pulse functions and two-variable shifted Legendre polynomials (2D-HBPSLs) and their operational matrices of product and fractional integration are introduced. Afterward, in Sect. 5, we explain numerical solutions of 2D-NFVIEs and 2D-NFFIEs, respectively, by using what was introduced in Sect. 4. Moreover, in Sect. 6, error bound and convergence analysis of the proposed method are discussed. To demonstrate the effectiveness of the presented method, three numerical examples are given in Sect. 7. Finally, in Sect. 8, a conclusion is given.

2 Preliminary knowledge

Here, we give two necessary definitions of the fractional calculus theory which are used throughout this paper.

Definition 1 (See Podlubony 1999) The Riemann–Liouville fractional integral of order $\alpha > 0$ is defined by

$$I_{\upsilon}^{\alpha} f(x) = \frac{1}{\Gamma(\alpha)} \int_{\upsilon}^{x} (x-\tau)^{\alpha-1} f(\tau) \mathrm{d}\tau,$$

where $\upsilon > 0$. If $\upsilon = 0$, for simplicity, we will denote the Riemann–Liouville fractional integral of order α of $f(x)$ with $I^{\alpha} f(x)$.

Definition 2 (See Abbas and Benchohra 2014) The left-sided mixed Riemann–Liouville fractional integral of order $\iota := (\iota_1, \iota_2) \in (0, \infty) \times (0, \infty)$ of f is defined by

$$I_{\sigma}^{\iota} f(x, y) = \frac{1}{\Gamma(\iota_1)\Gamma(\iota_2)} \int_{\sigma_1}^{x} \int_{\sigma_2}^{y} (x-\tau)^{\iota_1 - 1} (y-\varsigma)^{\iota_2 - 1} f(\tau, \varsigma) \mathrm{d}\varsigma \mathrm{d}\tau,$$

where $\sigma = (\sigma_1, \sigma_2)$. If $\sigma = (0, 0)$, for simplicity, we will denote the left-sided mixed Riemann–Liouville fractional integral of order ι of $f(x, y)$ with $I^{\iota} f(x, y)$.

3 Existence and uniqueness of solutions

In this section, we provide sufficient conditions for the existence and uniqueness of solutions for 2D-NFVIEs (1) and 2D-NFFIEs (2) in a Banach space. To do this, we need the following theorems.

Theorem 1 (The Arzela-Ascoli theorem (Conway 2007)) *If E is compact and $B \subseteq C(E)$, then B is totally bounded if and only if B is bounded and equicontinuous.*

Corollary 1 (See Conway 2007) *If E is compact and $B \subseteq C(E)$, then B is compact if and only if B is bounded, closed, and equicontinuous.*

Theorem 2 (Schauder's fixed-point theorem (Zeidler 1995)) *If Π_0 is a bounded, closed, convex, nonempty subset of a Banach space V and $T : \Pi_0 \to \Pi_0$ is completely continuous, then T has a fixed point.*

Theorem 3 (Tychonoff's fixed-point theorem (Zeidler 1995)) *Let V be a complete, locally convex, linear space and V_0 be a closed, convex, nonempty subset of V. Assume that the mapping $T : V \to V$ is continuous and $T(V_0) \subset V_0$. If the closure of $T(V_0)$ is compact, then T has a fixed point in V_0.*

In the following theorem, we prove the local existence of the solutions for 2D-NFVIEs using Schauder's fixed-point theorem.

Theorem 4 *Assume that*

(C1) *$f, v, g, g_1 \in C(\Omega, \mathbb{R}^n)$ and $k \in C(\Omega \times \Omega \times \mathbb{R}^n, \mathbb{R}^n)$, for $0 \leq \tau \leq x \leq \ell_1$ and $0 \leq \varsigma \leq y \leq \ell_2$.*
(C2) *$|g(x, y) - g_1(x, y)| < \frac{\varepsilon}{2}$.*

(C3) $|k(x,y,\tau,\varsigma,f(\tau,\varsigma)) - k(x,y,\tau,\varsigma,v(\tau,\varsigma))| < \frac{\varepsilon\Gamma(1+\iota_1)\Gamma(1+\iota_2)}{2\alpha^{\iota_1}\beta^{\iota_2}}$, *for some* $0<\alpha<\ell_1$ *and* $0<\beta<\ell_2$.

Then, the 2D-NFVIE has at least one solution on $0\le x\le\alpha,\ 0\le y\le\beta$.

Proof Consider the set $D=\{(x,y,\tau,\varsigma,f) : (x,y,\tau,\varsigma)\in\Omega\times\Omega, |f|\le b\}$. Let $|g(x,y)|\le\frac{b}{2}$ and $|k(x,y,\tau,\varsigma,f(\tau,\varsigma))|\le\xi$ on D. Choose $\frac{\xi\alpha^{\iota_1}\beta^{\iota_2}}{\Gamma(1+\iota_1)\Gamma(1+\iota_2)}\le\frac{b}{2}$ and let $\Pi_0=\{f : f\in C(\Omega_0,\mathbb{R}^n),\ \|f\|\le b\}$, where $\|f\|=\max_{(x,y)\in\Omega_0}|f(x,y)|$ and $\Omega_0=[0,\alpha]\times[0,\beta]$. Clearly, the set Π_0 is bounded, closed, and convex.

For any $f\in\Pi_0$, define the operator

$$Tf(x,y)=g(x,y)+\frac{1}{\Gamma(\iota_1)\Gamma(\iota_2)}\int_0^x\int_0^y(x-\tau)^{\iota_1-1}(y-\varsigma)^{\iota_2-1}k(x,y,\tau,\varsigma,f(\tau,\varsigma))\mathrm{d}\varsigma\mathrm{d}\tau,\quad (x,y)\in\Omega_0. \tag{3}$$

Clearly, we have

$$\begin{aligned}|Tf(x,y)|&\le|g(x,y)|\\&\quad+\frac{1}{\Gamma(\iota_1)\Gamma(\iota_2)}\int_0^x\int_0^y(x-\tau)^{\iota_1-1}(y-\varsigma)^{\iota_2-1}\,|k(x,y,\tau,\varsigma,f(\tau,\varsigma))|\,\mathrm{d}\varsigma\mathrm{d}\tau\\&\le\frac{b}{2}+\frac{\xi}{\Gamma(\iota_1)\Gamma(\iota_2)}\int_0^x\int_0^y(x-\tau)^{\iota_1-1}(y-\varsigma)^{\iota_2-1}\mathrm{d}\varsigma\mathrm{d}\tau\\&\le\frac{b}{2}+\frac{\xi\alpha^{\iota_1}\beta^{\iota_2}}{\Gamma(1+\iota_1)\Gamma(1+\iota_2)}\le b.\end{aligned}$$

Therefore, we obtain $\|Tf\|\le b$, which implies that $T(\Pi_0)\subset\Pi_0$. Furthermore, for any $(x_1,y_1),\ (x_2,y_2)\in\Omega_0$ such that $x_2>x_1$ and $y_2>y_1$, we have

$$\begin{aligned}Tf(x_2,y_2)-Tf(x_1,y_1)&=g(x_2,y_2)-g(x_1,y_1)\\&\quad+\frac{1}{\Gamma(\iota_1)\Gamma(\iota_2)}\int_0^{x_2}\int_0^{y_2}(x_2-\tau)^{\iota_1-1}(y_2-\varsigma)^{\iota_2-1}k(x_2,y_2,\tau,\varsigma,f(\tau,\varsigma))\mathrm{d}\varsigma\mathrm{d}\tau\\&\quad-\frac{1}{\Gamma(\iota_1)\Gamma(\iota_2)}\int_0^{x_1}\int_0^{y_1}(x_1-\tau)^{\iota_1-1}(y_1-\varsigma)^{\iota_2-1}k(x_1,y_1,\tau,\varsigma,f(\tau,\varsigma))\mathrm{d}\varsigma\mathrm{d}\tau\\&=g(x_2,y_2)-g(x_1,y_1)\\&\quad+\frac{1}{\Gamma(\iota_1)\Gamma(\iota_2)}\int_0^{x_1}\int_0^{y_1}(x_2-\tau)^{\iota_1-1}(y_2-\varsigma)^{\iota_2-1}k(x_2,y_2,\tau,\varsigma,f(\tau,\varsigma))\mathrm{d}\varsigma\mathrm{d}\tau\\&\quad+\frac{1}{\Gamma(\iota_1)\Gamma(\iota_2)}\int_{x_1}^{x_2}\int_{y_1}^{y_2}(x_2-\tau)^{\iota_1-1}(y_2-\varsigma)^{\iota_2-1}k(x_2,y_2,\tau,\varsigma,f(\tau,\varsigma))\mathrm{d}\varsigma\mathrm{d}\tau\\&\quad-\frac{1}{\Gamma(\iota_1)\Gamma(\iota_2)}\int_0^{x_1}\int_0^{y_1}(x_1-\tau)^{\iota_1-1}(y_1-\varsigma)^{\iota_2-1}k(x_1,y_1,\tau,\varsigma,f(\tau,\varsigma))\mathrm{d}\varsigma\mathrm{d}\tau\\&=g(x_2,y_2)-g(x_1,y_1)\\&\quad+\frac{1}{\Gamma(\iota_1)\Gamma(\iota_2)}\int_0^{x_1}\int_0^{y_1}\Big((x_2-\tau)^{\iota_1-1}(y_2-\varsigma)^{\iota_2-1}k(x_2,y_2,\tau,\varsigma,f(\tau,\varsigma))\\&\quad-(x_1-\tau)^{\iota_1-1}(y_1-\varsigma)^{\iota_2-1}k(x_1,y_1,\tau,\varsigma,f(\tau,\varsigma))\Big)\,\mathrm{d}\varsigma\mathrm{d}\tau\\&\quad+\frac{1}{\Gamma(\iota_1)\Gamma(\iota_2)}\int_{x_1}^{x_2}\int_{y_1}^{y_2}(x_2-\tau)^{\iota_1-1}(y_2-\varsigma)^{\iota_2-1}k(x_2,y_2,\tau,\varsigma,f(\tau,\varsigma))\mathrm{d}\varsigma\mathrm{d}\tau.\end{aligned} \tag{4}$$

Now adding and subtracting $(x_2-\tau)^{\iota_1-1}(y_2-\varsigma)^{\iota_2-1}k(x_1,y_1,\tau,\varsigma,f(\tau,\varsigma))$ to the right-hand side of the inequality (4) yields

$$\begin{aligned}
&Tf(x_2,y_2)-Tf(x_1,y_1)=g(x_2,y_2)-g(x_1,y_1)\\
&\quad+\frac{1}{\Gamma(\iota_1)\Gamma(\iota_2)}\int_0^{x_1}\int_0^{y_1}\big((x_2-\tau)^{\iota_1-1}(y_2-\varsigma)^{\iota_2-1}k(x_2,y_2,\tau,\varsigma,f(\tau,\varsigma))\\
&\quad-(x_2-\tau)^{\iota_1-1}(y_2-\varsigma)^{\iota_2-1}k(x_1,y_1,\tau,\varsigma,f(\tau,\varsigma))\\
&\quad+(x_2-\tau)^{\iota_1-1}(y_2-\varsigma)^{\iota_2-1}k(x_1,y_1,\tau,\varsigma,f(\tau,\varsigma))\\
&\quad-(x_1-\tau)^{\iota_1-1}(y_1-\varsigma)^{\iota_2-1}k(x_1,y_1,\tau,\varsigma,f(\tau,\varsigma))\big)\,\mathrm{d}\varsigma\mathrm{d}\tau\\
&\quad+\frac{1}{\Gamma(\iota_1)\Gamma(\iota_2)}\int_{x_1}^{x_2}\int_{y_1}^{y_2}(x_2-\tau)^{\iota_1-1}(y_2-\varsigma)^{\iota_2-1}k(x_2,y_2,\tau,\varsigma,f(\tau,\varsigma))\mathrm{d}\varsigma\mathrm{d}\tau\\
&=g(x_2,y_2)-g(x_1,y_1)\\
&\quad+\frac{1}{\Gamma(\iota_1)\Gamma(\iota_2)}\int_0^{x_1}\int_0^{y_1}\big((x_2-\tau)^{\iota_1-1}(y_2-\varsigma)^{\iota_2-1}\,(k(x_2,y_2,\tau,\varsigma,f(\tau,\varsigma))\\
&\quad-k(x_1,y_1,\tau,\varsigma,f(\tau,\varsigma)))\\
&\quad+k(x_1,y_1,\tau,\varsigma,f(\tau,\varsigma))\big((x_2-\tau)^{\iota_1-1}(y_2-\varsigma)^{\iota_2-1}\\
&\quad-(x_1-\tau)^{\iota_1-1}(y_1-\varsigma)^{\iota_2-1}\big)\big)\,\mathrm{d}\varsigma\mathrm{d}\tau\\
&\quad+\frac{1}{\Gamma(\iota_1)\Gamma(\iota_2)}\int_{x_1}^{x_2}\int_{y_1}^{y_2}(x_2-\tau)^{\iota_1-1}(y_2-\varsigma)^{\iota_2-1}k(x_2,y_2,\tau,\varsigma,f(\tau,\varsigma))\mathrm{d}\varsigma\mathrm{d}\tau.
\end{aligned}$$

Let

$$\begin{aligned}
|k(x_1,y_1,\tau,\varsigma,f(\tau,\varsigma))|&\le\eta_1,\\
|k(x_2,y_2,\tau,\varsigma,f(\tau,\varsigma))|&\le\eta_2,
\end{aligned}$$

and

$$|k(x_2,y_2,\tau,\varsigma,f(\tau,\varsigma))-k(x_1,y_1,\tau,\varsigma,f(\tau,\varsigma))|\le\eta_3,$$

for $(\tau,\varsigma)\in\Omega$, then we can write

$$\begin{aligned}
&|Tf(x_2,y_2)-Tf(x_1,y_1)|\le|g(x_2,y_2)-g(x_1,y_1)|\\
&\quad+\frac{1}{\Gamma(\iota_1)\Gamma(\iota_2)}\int_0^{x_1}\int_0^{y_1}\big((\eta_1+\eta_3)(x_2-\tau)^{\iota_1-1}(y_2-\varsigma)^{\iota_2-1}\\
&\quad+\eta_1(x_1-\tau)^{\iota_1-1}(y_1-\varsigma)^{\iota_2-1}\big)\,\mathrm{d}\varsigma\mathrm{d}\tau\\
&\quad+\frac{1}{\Gamma(\iota_1)\Gamma(\iota_2)}\int_{x_1}^{x_2}\int_{y_1}^{y_2}\eta_2(x_2-\tau)^{\iota_1-1}(y_2-\varsigma)^{\iota_2-1}\mathrm{d}\varsigma\mathrm{d}\tau\\
&=|g(x_2,y_2)-g(x_1,y_1)|+\frac{1}{\Gamma(1+\iota_1)\Gamma(1+\iota_2)}\big((\eta_1+\eta_3-\eta_2)(x_2-x_1)^{\iota_1}(y_2-y_1)^{\iota_2}\\
&\quad-(\eta_1+\eta_3)x_2^{\iota_1}y_2^{\iota_2}-\eta_1x_1^{\iota_1}y_1^{\iota_2}\big)\\
&\le|g(x_2,y_2)-g(x_1,y_1)|+\frac{\eta_1+\eta_3}{\Gamma(1+\iota_1)\Gamma(1+\iota_2)}(x_2-x_1)^{\iota_1}(y_2-y_1)^{\iota_2}.
\end{aligned}\tag{5}$$

Note that the right-hand side in the inequality (5) tends to zero as $x_2\to x_1$, $y_2\to y_1$. Therefore, $T:\Pi_0\to\Pi_0$ is equicontinuous and consequently, from Theorem 1, the closure of $T(\Pi_0)$ is compact.

To show that T is a continuous map, let

$$\begin{aligned} Tv(x,y) &= g_1(x,y) \\ &\quad + \frac{1}{\Gamma(\iota_1)\Gamma(\iota_2)} \int_0^x \int_0^y (x-\tau)^{\iota_1-1}(y-\varsigma)^{\iota_2-1} k(x,y,\tau,\varsigma,v(\tau,\varsigma)) \mathrm{d}\varsigma \mathrm{d}\tau, \end{aligned}$$

where $v \in \Pi_0$. Clearly, we have

$$\begin{aligned} &|Tf(x,y) - Tv(x,y)| \le |g(x,y) - g_1(x,y)| \\ &+ \frac{1}{\Gamma(\iota_1)\Gamma(\iota_2)} \int_0^x \int_0^y (x-\tau)^{\iota_1-1}(y-\varsigma)^{\iota_2-1} \,|k(x,y,\tau,\varsigma,f(\tau,\varsigma)) \\ &-k(x,y,\tau,\varsigma,v(\tau,\varsigma))| \,\mathrm{d}\varsigma \mathrm{d}\tau. \end{aligned}$$

Since k is uniformly continuous, for an arbitrary $\varepsilon > 0$, there exists a $\delta > 0$ such that $|f(x,y) - v(x,y)| < \delta$. Assume that conditions (**C1**)–(**C3**) are satisfied, then we obtain

$$\begin{aligned} &|Tf(x,y) - Tv(x,y)| \le \frac{\varepsilon}{2} \\ &+ \frac{1}{\Gamma(\iota_1)\Gamma(\iota_2)} \frac{\varepsilon \Gamma(1+\iota_1)\Gamma(1+\iota_2)}{2\alpha^{\iota_1}\beta^{\iota_2}} \int_0^x \int_0^y (x-\tau)^{\iota_1-1}(y-\varsigma)^{\iota_2-1} \mathrm{d}\varsigma \mathrm{d}\tau \le \varepsilon, \end{aligned}$$

and the proof is completed. □

We shall next discuss a global existence result for the 2D-NFVIEs using Tychonoff's fixed-point theorem.

Theorem 5 *Assume that*

(D1) $k \in C(\mathbb{R}_+^4 \times \mathbb{R}^n, \mathbb{R}^n)$ *and* $G \in C(\mathbb{R}_+^5, \mathbb{R}^n)$.
(D2) $G(x,y,\tau,\varsigma,u)$ *is monotone nondecreasing in* u*, for each* $(x,y,\tau,\varsigma) \in \mathbb{R}_+^4$.
(D3) $|k(x,y,\tau,\varsigma,f)| \le G(x,y,\tau,\varsigma,|f|)$*, for* $(x,y,\tau,\varsigma,f) \in \mathbb{R}_+^4 \times \mathbb{R}^n$.

Then, the fractional integral equation

$$\begin{aligned} u(x,y) &= q(x,y) \\ &\quad + \frac{1}{\Gamma(\iota_1)\Gamma(\iota_2)} \int_0^x \int_0^y (x-\tau)^{\iota_1-1}(y-\varsigma)^{\iota_2-1} G(x,y,\tau,\varsigma,u(\tau,\varsigma)) \mathrm{d}\varsigma \mathrm{d}\tau, \quad (6) \end{aligned}$$

has a solution $u(x,y)$*, for every* $x, y \ge 0$*, and then for every* $q(x,y) \in \mathbb{R}_+^2$ *such that* $|g(x,y)| \le q(x,y)$*, there exists a solution* $f(x,y)$ *for 2D-NFVIE satisfying* $|f(x,y)| \le u(x,y)$.

Proof Assume that the real vector space V consists of all continuous functions from $(0,\infty) \times (0,\infty)$ into $\mathbb{R}^n$. The topology on V being that induced by the family of pseudo-norms $\{V_{n,m}(f)\}_{n,m=1}^{\infty}$, where $V_{n,m}(f) = \sup_{0 \le x \le n, 0 \le y \le m} |f(x,y)|$, for $f \in V$. Let $\{S_{n,m}\}_{n,m=1}^{\infty}$ be a fundamental system of neighborhoods, where $S_{n,m} = \{f \in V : V_{n,m}(f) \le 1\}$. Under this topology, V is complete and locally convex linear space.

Now define the subset V_0 of V as follows:

$$V_0 = \{f \in V : |f(x,y)| \le u(x,y),\ x,y \ge 0\} \subseteq V,$$

where $u(x,y)$ is a solution of Eq. (6). It is clear that in the topology of V, V_0 is closed, convex, and bounded.

Consider the Eq. (6) whose fixed point corresponds to a solution of Eq. (1). Evidently, in the topology of V, the operator T is compact. Hence, in view of the boundedness of V_0, the closure of $T(V_0)$ is compact.

Now using conditions (**D1**)–(**D3**), we observe that for any $f \in V_0$,

$$\begin{aligned} |Tf(x,y)| &\leq |g(x,y)| \\ &\quad + \frac{1}{\Gamma(\iota_1)\Gamma(\iota_2)} \int_0^x \int_0^y (x-\tau)^{\iota_1-1}(y-\varsigma)^{\iota_2-1} \left|k(x,y,\tau,\varsigma,f(\tau,\varsigma))\right| \mathrm{d}\varsigma \mathrm{d}\tau \\ &\leq |g(x,y)| + \frac{1}{\Gamma(\iota_1)\Gamma(\iota_2)} \int_0^x \int_0^y (x-\tau)^{\iota_1-1}(y-\varsigma)^{\iota_2-1} G(x,y,\tau,\varsigma,|f(\tau,\varsigma)|) \mathrm{d}\varsigma \mathrm{d}\tau \\ &\leq q(x,y) \\ &\quad + \frac{1}{\Gamma(\iota_1)\Gamma(\iota_2)} \int_0^x \int_0^y (x-\tau)^{\iota_1-1}(y-\varsigma)^{\iota_2-1} G(x,y,\tau,\varsigma,u(\tau,\varsigma)) \mathrm{d}\varsigma \mathrm{d}\tau = u(x,y). \end{aligned}$$

It is clear that using the fact that $u(x,y)$ is a solution of 2D-NFVIE and from the definition of V_0, we can obtain $|Tf(x,y)| \leq u(x,y)$, which implies that $T(V_0) \subset V_0$. Therefore, by Tychonoff's fixed-point theorem, the mapping T has a fixed point in V_0, which completes the proof of this theorem. □

In the following theorem, we prove the uniqueness of the solution for 2D-NFVIEs.

Theorem 6 *Let $f \in C(\Omega, \mathbb{R}^n)$ and $k \in C(\Omega \times \Omega \times \mathbb{R}^n, \mathbb{R}^n)$. Suppose that there exists $0 < L_1 < 1$ such that the following Lipschitz condition is satisfied:*

$$|k(x,y,\tau,\varsigma,f(\tau,\varsigma)) - k(x,y,\tau,\varsigma,f_1(\tau,\varsigma))| \leq L_1 \left|f(\tau,\varsigma) - f_1(\tau,\varsigma)\right|.$$

If $\frac{L_1 \ell_1^{\iota_1} \ell_2^{\iota_2}}{\Gamma(\iota_1+1)\Gamma(\iota_2+1)} < 1$, then the 2D-NFVIE has a unique solution.

Proof Let

$$\begin{aligned} Tf(x,y) &= g(x,y) \\ &\quad + \frac{1}{\Gamma(\iota_1)\Gamma(\iota_2)} \int_0^x \int_0^y (x-\tau)^{\iota_1-1}(y-\varsigma)^{\iota_2-1} k(x,y,\tau,\varsigma,f(\tau,\varsigma)) \mathrm{d}\varsigma \mathrm{d}\tau, \quad (x,y) \in \Omega, \end{aligned}$$

then, for any $f, \ f_1 \in C(\Omega, \mathbb{R}^n)$ and $(x,y) \in \Omega$, we have

$$\begin{aligned} &|Tf(x,y) - Tf_1(x,y)| \\ &= \Bigg| g(x,y) + \frac{1}{\Gamma(\iota_1)\Gamma(\iota_2)} \int_0^x \int_0^y (x-\tau)^{\iota_1-1}(y-\varsigma)^{\iota_2-1} k(x,y,\tau,\varsigma,f(\tau,\varsigma)) \mathrm{d}\varsigma \mathrm{d}\tau \\ &\quad - g(x,y) - \frac{1}{\Gamma(\iota_1)\Gamma(\iota_2)} \int_0^x \int_0^y (x-\tau)^{\iota_1-1}(y-\varsigma)^{\iota_2-1} k(x,y,\tau,\varsigma,f_1(\tau,\varsigma)) \mathrm{d}\varsigma \mathrm{d}\tau \Bigg| \\ &\leq \frac{1}{\Gamma(\iota_1)\Gamma(\iota_2)} \int_0^x \int_0^y (x-\tau)^{\iota_1-1}(y-\varsigma)^{\iota_2-1} \left|k(x,y,\tau,\varsigma,f(\tau,\varsigma)) \right. \\ &\quad \left. - k(x,y,\tau,\varsigma,f_1(\tau,\varsigma))\right| \mathrm{d}\varsigma \mathrm{d}\tau \\ &\leq \frac{L_1}{\Gamma(\iota_1)\Gamma(\iota_2)} \int_0^x \int_0^y (x-\tau)^{\iota_1-1}(y-\varsigma)^{\iota_2-1} \left|f(\tau,\varsigma) - f_1(\tau,\varsigma)\right| \mathrm{d}\varsigma \mathrm{d}\tau \\ &\leq \frac{L_1 \ell_1^{\iota_1} \ell_2^{\iota_2}}{\Gamma(\iota_1+1)\Gamma(\iota_2+1)} \left\|f - f_1\right\|. \end{aligned}$$

Therefore,

$$\|Tf - Tf_1\| \leq \frac{L_1 \ell_1^{\iota_1} \ell_2^{\iota_2}}{\Gamma(\iota_1+1)\Gamma(\iota_2+1)} \|f - f_1\|.$$

Since $\frac{L_1 \ell_1^{\iota_1} \ell_2^{\iota_2}}{\Gamma(\iota_1+1)\Gamma(\iota_2+1)} < 1$, it follows that T is a contraction in $C(\Omega, \mathbb{R}^n)$. Consequently, T has a unique fixed point and therefore the 2D-NFVIE has a unique solution $f \in C(\Omega, \mathbb{R}^n)$. □

Now, in the following theorems, we are going to investigate a result of the existence and uniqueness of the solution for 2D-NFFIEs.

Theorem 7 *Assume that conditions (**C1**)–(**C3**) in Theorem 4 hold. Then the 2D-NFFIE has at least one solution on* $0 \leq x \leq \alpha,\ 0 \leq y \leq \beta$.

Proof The proof of this theorem is similar to the proof of Theorem 4. □

Theorem 8 *Assume that conditions (**D1**)–(**D3**) in Theorem 5 hold. Then, the fractional integral equation*

$$u(x, y) = q(x, y) + \frac{1}{\Gamma(\iota_1)\Gamma(\iota_2)} \int_0^{\ell_1} \int_0^{\ell_2} (\ell_1 - \tau)^{\iota_1 - 1} (\ell_2 - \varsigma)^{\iota_2 - 1} G(x, y, \tau, \varsigma, u(\tau, \varsigma)) \mathrm{d}\varsigma \mathrm{d}\tau, \tag{7}$$

has a solution $u(x, y)$ existing for every $x, y \geq 0$, and then for every $q(x, y) \in \mathbb{R}_+^2$, such that $|g(x, y)| \leq q(x, y)$, there exists a solution $f(x, y)$ of the 2D-NFFIE for $x, y \geq 0$ satisfying $|f(x, y)| \leq u(x, y)$.

Proof The proof of this theorem is similar to the proof of Theorem 5. □

Theorem 9 *Let $f \in C(\Omega, \mathbb{R}^n)$ and $k \in C(\Omega \times \Omega \times \mathbb{R}^n, \mathbb{R}^n)$. Suppose that there exists $0 < L_2 < 1$ such that the following Lipschitz condition is satisfied:*

$$|k(x, y, \tau, \varsigma, f(\tau, \varsigma)) - k(x, y, \tau, \varsigma, f_1(\tau, \varsigma))| \leq L_2 |f(\tau, \varsigma) - f_1(\tau, \varsigma)|.$$

If $\frac{L_2 \ell_1^{\iota_1} \ell_2^{\iota_2}}{\Gamma(\iota_1+1)\Gamma(\iota_2+1)} < 1$, then the 2D-NFFIE has a unique solution.

Proof The proof of this theorem is similar to the proof of Theorem 6. □

4 The 2D-HBPSLs and the operational matrices

Here, we present the 2D-HBPSLs and use them to obtain the approximation of two-variable functions. Then, we review the operational matrices of fractional integration and product.

First, consider the 1D-HBPSLs on the interval $[0, \ell)$ as follows:

$$\hbar_{nm}(x) = \begin{cases} \phi_m(\frac{2N}{\ell}x - 2n + 1), & x \in [\frac{n-1}{N}\ell, \frac{n}{N}\ell), \\ 0, & \text{otherwise}, \end{cases}$$

for $n = 1, 2, \ldots, N,\ m = 0, 1, \ldots, M - 1$, where N and M are positive integers. Here, ϕ_m is Legendre polynomial of degree m which is defined on $[-1, 1]$ with the analytic form

$$\phi_m(x) = 2^m \sum_{j=0}^{m} x^j \binom{m}{j} \binom{\frac{m+j-1}{2}}{m}.$$

The orthogonality property of the 1D-HBPSLs on the interval $[0, \ell)$ is as follows:

$$\int_0^{\ell} \hbar_{nm}(x)\hbar_{ij}(x)\mathrm{d}x = \begin{cases} \frac{\ell}{N(2m+1)}, & n=i, m=j, \\ 0, & \text{otherwise.} \end{cases}$$

Similarly, the 2D-HBPSLs on the domain $\Omega = [0, \ell_1) \times [0, \ell_2)$ is defined as follows:

$$\hbar_{n_1m_1n_2m_2}(x, y) = \begin{cases} \phi_{m_1}\left(\frac{2N}{\ell_1}x - 2n_1 + 1\right)\phi_{m_2}\left(\frac{2N}{\ell_2}y - 2n_2 + 1\right), & (x, y) \in [\frac{n_1-1}{N}\ell_1, \frac{n_1}{N}\ell_1) \times [\frac{n_2-1}{N}\ell_2, \frac{n_2}{N}\ell_2), \\ 0, & \text{otherwise.} \end{cases}$$

Here ϕ_{m_1} and ϕ_{m_2} are Legendre polynomials of degrees m_1 and m_2, respectively, where $n_1, n_2 = 1, 2, \ldots, N,\ m_1, m_2 = 0, 1, \ldots, M-1$.

The orthogonality property of the 2D-HBPSLs on the domain Ω is

$$\int_0^{\ell_1}\int_0^{\ell_2} \hbar_{n_1m_1n_2m_2}(x, y)\hbar_{i_1j_1i_2j_2}(x, y)\,\mathrm{d}y\,\mathrm{d}x = \begin{cases} \frac{\ell_1\ell_2}{N^2(2m_1+1)(2m_2+1)}, & n_1=i_1, n_2=i_2, m_1=j_1, m_2=j_2, \\ 0, & \text{otherwise.} \end{cases}$$

Now consider the space $X = L^2(\Omega)$ with the norm

$$\|f\|_2 = \langle f, f\rangle^{\frac{1}{2}} = \left(\int_0^{\ell_1}\int_0^{\ell_2} |f(x, y)|^2\,\mathrm{d}y\mathrm{d}x\right)^{\frac{1}{2}},$$

where $\langle ., .\rangle$ denotes the inner product. Let

$$X_{N,M} = span\{\hbar_{1010}(x, y), \ldots, \hbar_{101(M-1)}(x, y), \hbar_{1020}(x, y), \ldots, \hbar_{102(M-1)}(x, y), \ldots, \hbar_{N(M-1)N0}(x, y), \ldots, \hbar_{N(M-1)N(M-1)}(x, y)\}.$$

Since $X_{N,M} \subset X$ is a finite dimensional vector space, for every $f \in X$ there exists a unique best approximation $f_{N,M} \in X_{N,M}$ such that

$$\left\|f - f_{N,M}\right\|_2 = \inf_{u \in X_{N,M}} \|f - u\|_2.$$

A proof of this result is given by Cheney (1966), Davis (1975), and Kreyszig (1989). Since $f_{N,M} \in X_{N,M}$, we have

$$f(x, y) \simeq f_{N,M}(x, y) = \sum_{n_1=1}^{N}\sum_{m_1=0}^{M-1}\sum_{n_2=1}^{N}\sum_{m_2=0}^{M-1} \hat{f}_{n_1m_1n_2m_2}\hbar_{n_1m_1n_2m_2}(x, y) = \hat{F}^T H(x, y), \tag{8}$$

where

$$\hat{F} = [\hat{f}_{1010}, \ldots, \hat{f}_{101(M-1)}, \hat{f}_{1020}, \ldots, \hat{f}_{102(M-1)}, \ldots, \hat{f}_{N(M-1)N0}, \ldots, \hat{f}_{N(M-1)N(M-1)}]^T, \tag{9}$$

$$H(x, y) = [\hbar_{1010}(x, y), \ldots, \hbar_{101(M-1)}(x, y), \hbar_{1020}(x, y), \ldots, \hbar_{102(M-1)}(x, y), \ldots, \hbar_{N(M-1)N0}(x, y), \ldots, \hbar_{N(M-1)N(M-1)}(x, y)]^T, \tag{10}$$

and hybrid coefficients are uniquely obtained by

$$\hat{f}_{n_1 m_1 n_2 m_2} = \frac{\langle f, \hbar_{n_1 m_1 n_2 m_2} \rangle}{\langle \hbar_{n_1 m_1 n_2 m_2}, \hbar_{n_1 m_1 n_2 m_2} \rangle}. \tag{11}$$

Now consider $X = L^2(\Omega \times \Omega)$ with

$$\|k\|_2 = \langle k, k \rangle^{\frac{1}{2}} = \left(\int_0^{\ell_1} \int_0^{\ell_2} \int_0^{\ell_1} \int_0^{\ell_2} |k(x, y, \tau, \varsigma)|^2 \, \mathrm{d}\varsigma \, \mathrm{d}\tau \, \mathrm{d}y \, \mathrm{d}x \right)^{\frac{1}{2}}.$$

Also, a function k in X can be expanded as follows:

$$k(x, y, \tau, \varsigma) \simeq H^T(x, y) K H(\tau, \varsigma), \tag{12}$$

where K is the $N^2M^2 \times N^2M^2$ known matrix and its entries are given by

$$K_{n,m} = \frac{\int_0^{\ell_1} \int_0^{\ell_2} \int_0^{\ell_1} \int_0^{\ell_2} H_{(n)}(x, y) k(x, y, \tau, \varsigma) H_{(m)}(\tau, \varsigma) \, \mathrm{d}\varsigma \, \mathrm{d}\tau \, \mathrm{d}y \, \mathrm{d}x}{\left(\int_0^{\ell_1} \int_0^{\ell_2} |H_{(n)}(x, y)|^2 \, \mathrm{d}y \, \mathrm{d}x \right) \left(\int_0^{\ell_1} \int_0^{\ell_2} |H_{(m)}(\tau, \varsigma)|^2 \, \mathrm{d}\varsigma \, \mathrm{d}\tau \right)}. \tag{13}$$

Here $H_{(n)}(x, y)$ denotes the nth element of $H(x, y)$.

4.1 The operational matrix of fractional integration

Maleknejad et al. (2020a) obtained the left-sided mixed Riemann–Liouville fractional integral of order $\iota := (\iota_1, \iota_2)$ of 2D-HBPSLs as follows:

$$I^{(\iota_1, \iota_2)} H(x, y) \simeq \left(\mathbf{I}^{\iota_1} \otimes \mathbf{I}^{\iota_2} \right) H(x, y). \tag{14}$$

Here, $\otimes$ denotes the Kronecker product and $\mathbf{I}^{\iota_1} \otimes \mathbf{I}^{\iota_2}$ is the operational matrix of fractional integration of 2D-HBPSLs, where

$$\mathbf{I}^{\iota_i} = \Psi \mathbf{P}^{\iota_i} \Psi^{-1}, \qquad i = 1, 2, \tag{15}$$

and

$$\mathbf{P}^{\iota_i} = \left(\frac{\ell_i}{NM} \right)^{\iota_i} \frac{1}{\Gamma(\iota_i + 2)} \begin{bmatrix} 1 & \kappa_1 & \kappa_2 & \dots & \kappa_{NM-1} \\ 0 & 1 & \kappa_1 & \dots & \kappa_{NM-2} \\ 0 & 0 & 1 & \dots & \kappa_{NM-3} \\ \vdots & \vdots & \vdots & \ddots & \vdots \\ 0 & 0 & 0 & \dots & 1 \end{bmatrix},$$

with $\kappa_l = (l+1)^{\iota_i+1} - 2l^{\iota_i+1} + (l-1)^{\iota_i+1}, l = 1, 2, \dots, NM-1$, is the operational matrix of fractional integration of block-pulse functions given by Kılıçman and Al Zhour (2007). Also, Ψ_i is an $NM \times NM$ matrix given by

$$\Psi_i \triangleq \left[H\left(\frac{\ell_i}{2NM} \right), H\left(\frac{3\ell_i}{2NM} \right), \dots, H\left(\frac{(2NM-1)\ell_i}{2NM} \right) \right]_{NM \times NM},$$

where

$$H(x) = [\hbar_{10}(x), \dots, \hbar_{1(M-1)}(x), \hbar_{20}(x), \dots, \hbar_{N(M-1)}(x)]^T,$$

is an $NM \times 1$ vector of 1D-HBPSLs.

Moreover, from Maleknejad et al. (2020a), we have

$$\frac{1}{\Gamma(\iota_1)\Gamma(\iota_2)}\int_0^{\ell_1}\int_0^{\ell_2}(\ell_1-\tau)^{\iota_1-1}(\ell_2-\varsigma)^{\iota_2-1}H(\tau,\varsigma)\mathrm{d}\varsigma\mathrm{d}\tau=\Xi_1\otimes\Xi_2, \tag{16}$$

where

$$\Xi_1=\frac{1}{\Gamma(\iota_1)}\int_0^{\ell_1}(\ell_1-\tau)^{\iota_1-1}H(\tau)\mathrm{d}\tau,$$

and

$$\Xi_2=\frac{1}{\Gamma(\iota_2)}\int_0^{\ell_2}(\ell_2-\varsigma)^{\iota_2-1}H(\varsigma)\mathrm{d}\varsigma.$$

4.2 The product operational matrix

Let $H(x, y)$ be the 2D-HBPSLs vector defined in (10), then we have

$$H(x,y)H^T(x,y)\hat{F}\simeq\tilde{\hat{F}}H(x,y), \tag{17}$$

where $\hat{F}$ is defined by (9) and $\tilde{\hat{F}}$ is an $N^2M^2\times N^2M^2$ product operational matrix. Maleknejad et al. (2020a) have computed the entries of $\tilde{\hat{F}}=diag(C_{i_1})_{i_1=1,2,\ldots,N}$ as follows:

$$\begin{aligned}
C_{i_1}&=\left[C_{i_1}^{(j_1,m_1)}\right]_{j_1,m_1=0,1,\ldots,M-1},\\
C_{i_1}^{(j_1,m_1)}&=\frac{N(2m_1+1)}{\ell_1}\sum_{h_1=0}^{M-1}w_{i_1j_1h_1m_1}B_{i_1h_1},\quad j_1,m_1=0,1,\ldots,M-1,\\
w_{i_1j_1h_1m_1}&=\int_{\frac{i_1-1}{N}\ell_1}^{\frac{i_1}{N}\ell_1}\phi_{j_1}\left(\frac{2N}{\ell_1}x-2i_1+1\right)\phi_{h_1}\left(\frac{2N}{\ell_1}x-2i_1+1\right)\phi_{m_1}\\
&\quad\times\left(\frac{2N}{\ell_1}x-2i_1+1\right)\mathrm{d}x,\\
B_{i_1h_1}&=\mathrm{diag}(A_{i_1,h_1,i_2})_{i_2=1,2,\ldots,N},\\
A_{i_1,h_1,i_2}&=\left[A_{i_1,h_1,i_2}^{(j_2,m_2)}\right]_{j_2,m_2=0,\ldots,M-1},\\
A_{i_1,h_1,i_2}^{(j_2,m_2)}&=\frac{N(2m_2+1)}{\ell_2}\sum_{h_2=0}^{M-1}w_{i_2j_2h_2m_2}\hat{f}_{i_1h_1i_2h_2},\quad j_2,m_2=0,\ldots,M-1,\\
w_{i_2j_2h_2m_2}&=\int_{\frac{i_2-1}{N}\ell_2}^{\frac{i_2}{N}\ell_2}\phi_{j_2}\left(\frac{2N}{\ell_2}y-2i_2+1\right)\phi_{h_2}\left(\frac{2N}{\ell_2}y-2i_2+1\right)\phi_{m_2}\\
&\quad\times\left(\frac{2N}{\ell_2}y-2i_2+1\right)\mathrm{d}y.
\end{aligned}$$

5 Method of solution

In this section, we suppose that $k(x, y, \tau, \varsigma, f(\tau, \varsigma)) = k(x, y, \tau, \varsigma)f^p(\tau, \varsigma)$ and then we use 2D-HBPSLs and their operational matrices for solving Eqs. (1) and (2).

5.1 The method for 2D-NFVIEs

Here, we are going to convert Eq. (1) to a nonlinear system using 2D-HBPSLs. First, we can write

$$g(x,y) \simeq H^T(x,y)G, \tag{18}$$

Using (8) and (17) for the function $f(x,y)$, we obtain

$$[f(x,y)]^2 \simeq \hat{F}^T H(x,y) H^T(x,y)\hat{F} = \underbrace{\hat{F}^T \tilde{\hat{F}}}_{\hat{F}_2} H(x,y) = \hat{F}_2 H(x,y),$$

$$[f(x,y)]^3 \simeq \hat{F}^T H(x,y)\hat{F}_2 H(x,y) = \hat{F}^T H(x,y) H^T(x,y)\hat{F}_2^T = \underbrace{\hat{F}^T \widetilde{\hat{F}_2^T}}_{\hat{F}_3} H(x,y)$$
$$= \hat{F}_3 H(x,y).$$

where $\widetilde{\hat{F}_2^T}$ is an $N^2M^2 \times N^2M^2$ product operational matrix. By expanding the method for an arbitrary $p \in \mathbb{N}$, the result is as follows:

$$[f(x,y)]^p \simeq \hat{F}_p H(x,y). \tag{19}$$

Now, using (8), (12), (14), (17) -(19), we get

$$\begin{aligned}
H^T(x,y)\hat{F} &\simeq H^T(x,y)G \\
&\quad + \frac{1}{\Gamma(\iota_1)\Gamma(\iota_2)} \int_0^x \int_0^y (x-\tau)^{\iota_1-1}(y-\varsigma)^{\iota_2-1} H^T(x,y) K H(\tau,\varsigma)\hat{F}_p H(\tau,\varsigma)\mathrm{d}\varsigma\mathrm{d}\tau \\
&\simeq H^T(x,y)G \\
&\quad + \frac{1}{\Gamma(\iota_1)\Gamma(\iota_2)} \int_0^x \int_0^y (x-\tau)^{\iota_1-1}(y-\varsigma)^{\iota_2-1} H^T(x,y) K \widetilde{\hat{F}_p^T} H(\tau,\varsigma)\mathrm{d}\varsigma\mathrm{d}\tau \\
&= H^T(x,y)G \\
&\quad + H^T(x,y) K \widetilde{\hat{F}_p^T} \left(\frac{1}{\Gamma(\iota_1)\Gamma(\iota_2)} \int_0^x \int_0^y (x-\tau)^{\iota_1-1}(y-\varsigma)^{\iota_2-1} H(\tau,\varsigma)\mathrm{d}\varsigma\mathrm{d}\tau \right) \\
&\simeq H^T(x,y)G + H^T(x,y) K \widetilde{\hat{F}_p^T} \left(\mathbf{I}^{\iota_1} \otimes \mathbf{I}^{\iota_2}\right) H(x,y).
\end{aligned}$$

Therefore, we have

$$H^T(x,y)\hat{F} \simeq H^T(x,y)G + H^T(x,y) K \widetilde{\hat{F}_p^T} \left(\mathbf{I}^{\iota_1} \otimes \mathbf{I}^{\iota_2}\right) H(x,y). \tag{20}$$

To obtain unknown coefficients $\hat{f}_{n_1 m_1 n_2 m_2}$, for $n_1, n_2 = 1, 2, \ldots, N$, $m_1, m_2 = 0, 1, \ldots, M-1$, we collocate Eq. (20) at N^2M^2 collocation points $\{(x_i, y_j)\}_{i,j=1}^{NM}$ in the domain $\Omega = [0, \ell_1) \times [0, \ell_2)$, where

$$x_i = \frac{2i-1}{2NM}, \; y_j = \frac{2j-1}{2NM}, \quad i, j = 1, 2, \ldots, NM,$$

are the Newton-Cotes nodes. Therefore, we have N^2M^2 nonlinear equations. By solving this system, we determine an approximate solution for 2D-NFVIE from (8).

5.2 The method for 2D-NFFIEs

Now we want to convert Eq. (2) to a nonlinear system using 2D-HBPSLs. For this purpose, we apply (8), (12), (16)–(19) in (2) and, therefore, we obtain

$$\begin{aligned}
H^T(x,y)\hat{F} &\simeq H^T(x,y)G \\
&\quad + \frac{1}{\Gamma(\iota_1)\Gamma(\iota_2)}\int_0^{\ell_1}\int_0^{\ell_2}(\ell_1-\tau)^{\iota_1-1}(\ell_2-\varsigma)^{\iota_2-1}H^T(x,y)KH(\tau,\varsigma)\hat{F}_pH(\tau,\varsigma)\mathrm{d}\varsigma\mathrm{d}\tau \\
&\simeq H^T(x,y)G \\
&\quad + \frac{1}{\Gamma(\iota_1)\Gamma(\iota_2)}\int_0^{\ell_1}\int_0^{\ell_2}(\ell_1-\tau)^{\iota_1-1}(\ell_2-\varsigma)^{\iota_2-1}H^T(x,y)K\widetilde{\hat{F}_p^T}H(\tau,\varsigma)\mathrm{d}\varsigma\mathrm{d}\tau \\
&= H^T(x,y)G \\
&\quad + H^T(x,y)K\widetilde{\hat{F}_p^T}\left(\frac{1}{\Gamma(\iota_1)\Gamma(\iota_2)}\int_0^{\ell_1}\int_0^{\ell_2}(\ell_1-\tau)^{\iota_1-1}(\ell_2-\varsigma)^{\iota_2-1}H(\tau,\varsigma)\mathrm{d}\varsigma\mathrm{d}\tau\right) \\
&\simeq H^T(x,y)G + H^T(x,y)K\widetilde{\hat{F}_p^T}(\Xi_1\otimes\Xi_2).
\end{aligned}$$

So, we have

$$H^T(x,y)\hat{F} \simeq H^T(x,y)G + H^T(x,y)K\widetilde{\hat{F}_p^T}(\Xi_1\otimes\Xi_2). \tag{21}$$

Obtaining the unknown coefficients $\hat{f}_{n_1m_1n_2m_2}$ in the above system is similar to (20). Therefore, we can determine an approximate solution for 2D-NFFIE from (8).

6 Error bound and convergence analysis

Theorem 10 *Suppose that $f \in C^{(2M)}(\Omega)$. Let $f(x,y)$ be the exact solution of the 2D-NFVIE and $f_{N,M}(x,y)$ be its approximate solution obtained by the proposed method. Assume that for $(x,y)\in\Omega=[0,\ell_1)\times[0,\ell_2)$, the following assumptions hold:*

(H1) *$g\in C^{(2M)}(\Omega)$ and $k\in C^{(4M)}(\Omega\times\Omega)$.*
(H2) *There exists a Lipschitz constant L such that*

$$\left|f^p(x,y)-f^p_{N,M}(x,y)\right| \le L\left|f(x,y)-f_{N,M}(x,y)\right|.$$

(H3) $\sup_{\Omega}|f^p(x,y)|=a'<\infty$.
(H4) $\sup_{\Omega\times\Omega}|k(x,y,\tau,\varsigma)|=b'<\infty$.

Then, there exist positive constants μ_1 and μ_2 such that

$$\|f-f_{N,M}\|_2 \le \left(\frac{c'\Gamma(\iota_1+1)\Gamma(\iota_2+1)+\mu_1\ell_1^{\iota_1}\ell_2^{\iota_2}}{\Gamma(\iota_1+1)\Gamma(\iota_2+1)-\mu_2\ell_1^{\iota_1}\ell_2^{\iota_2}}\right)\frac{\sqrt{\ell_1\ell_2}}{2^{2M-1}N^MM!}. \tag{22}$$

Proof Considering the two-dimensional hybrid expansions of $f(x,y)$ and $k(x,y,\tau,\varsigma)$ and also using assumptions (**H1**)–(**H4**) lead to

$$\begin{aligned}
\left|f(x,y)-f_{N,M}(x,y)\right| &= \Big|g(x,y)-g_{N,M}(x,y) \\
&\quad + \frac{1}{\Gamma(\iota_1)\Gamma(\iota_2)}\int_0^{x}\int_0^{y}(x-\tau)^{\iota_1-1}(y-\varsigma)^{\iota_2-1}k(x,y,\tau,\varsigma)f^p(\tau,\varsigma)\mathrm{d}\varsigma\mathrm{d}\tau
\end{aligned}$$

$$
\begin{aligned}
&-\frac{1}{\Gamma(\iota_1)\Gamma(\iota_2)}\int_0^x\int_0^y (x-\tau)^{\iota_1-1}(y-\varsigma)^{\iota_2-1}k_{N,M}(x,y,\tau,\varsigma)f^p_{N,M}(\tau,\varsigma)\mathrm{d}\varsigma\mathrm{d}\tau\Bigg| \\
&\le \left|g(x,y)-g_{N,M}(x,y)\right| \\
&\quad+\left|\frac{1}{\Gamma(\iota_1)\Gamma(\iota_2)}\int_0^x\int_0^y (x-\tau)^{\iota_1-1}(y-\varsigma)^{\iota_2-1}\Big(k(x,y,\tau,\varsigma)\left(f^p(\tau,\varsigma)-f^p_{N,M}(\tau,\varsigma)\right)\right. \\
&\quad\left.+\left(k(x,y,\tau,\varsigma)-k_{N,M}(x,y,\tau,\varsigma)\right)f^p_{N,M}(\tau,\varsigma)\Big)\mathrm{d}\varsigma\mathrm{d}\tau\right| \\
&\le \left|g(x,y)-g_{N,M}(x,y)\right| \\
&\quad+\frac{1}{\Gamma(\iota_1)\Gamma(\iota_2)}\int_0^x\int_0^y (x-\tau)^{\iota_1-1}(y-\varsigma)^{\iota_2-1}\Big(b'L\left|f(\tau,\varsigma)-f_{N,M}(\tau,\varsigma)\right| \\
&\quad+a'\left|k(x,y,\tau,\varsigma)-k_{N,M}(x,y,\tau,\varsigma)\right|\Big)\mathrm{d}\varsigma\mathrm{d}\tau.
\end{aligned}\tag{23}
$$

Now from Maleknejad et al. (2020a) (see Theorem 6, page 16), we can write

$$
\left\|g-g_{N,M}\right\|_2 \le \frac{c'\sqrt{\ell_1\ell_2}}{2^{2M-1}N^M M!},
$$

and

$$
\|k-k_{N,M}\|_2 \le \frac{d'\sqrt{\ell_1\ell_2}}{2^{2M-1}N^M M!}.
$$

Also, by taking L^2-norm in the inequality (23), we obtain

$$
\begin{aligned}
\|f-f_{N,M}\|_2 &\le \left\|g-g_{N,M}\right\|_2 \\
&\quad+\frac{\ell_1^{\iota_1}\ell_2^{\iota_2}}{\Gamma(\iota_1+1)\Gamma(\iota_2+1)}\left(b'L\|f-f_{N,M}\|_2+a'\left\|k-k_{N,M}\right\|_2\right) \\
&\le \frac{c'\sqrt{\ell_1\ell_2}}{2^{2M-1}N^M M!} \\
&\quad+\frac{\ell_1^{\iota_1}\ell_2^{\iota_2}}{\Gamma(\iota_1+1)\Gamma(\iota_2+1)}\left(b'L\|f-f_{N,M}\|_2+\frac{a'd'\sqrt{\ell_1\ell_2}}{2^{2M-1}N^M M!}\right) \\
&\le \left(c'+\frac{a'd'\ell_1^{\iota_1}\ell_2^{\iota_2}}{\Gamma(\iota_1+1)\Gamma(\iota_2+1)}\right)\frac{\sqrt{\ell_1\ell_2}}{2^{2M-1}N^M M!} \\
&\quad+\frac{b'L\ell_1^{\iota_1}\ell_2^{\iota_2}}{\Gamma(\iota_1+1)\Gamma(\iota_2+1)}\|f-f_{N,M}\|_2.
\end{aligned}
$$

By simplifying the above relation and also setting $\mu_1 = a'd'$ and $\mu_2 = b'L$, we get the inequality (22) which completes the proof of the theorem. □

Remark 1 To obtain an upper error bound for 2D-NFFIEs, since $(x, y) \in \Omega$, we can use a similar way that has been used in Theorem 10.

Remark 2 It is obvious that the right-hand side of the inequality (22) tends to zero as $N, M \to \infty$, so $f - f_{N,M} \to 0$ and this proves the convergence of the proposed method.

7 Illustrative examples

In this section, we present three examples to demonstrate the accuracy and efficiency of the proposed method. In all these examples, $\hat{n}$ denotes the number of bases. All examples are

Table 1 Numerical results for Example 1

$x = y$	Exact solution	Present method		2D-SLPM		2D-BPFs	
		$M = 2$	$M = 3$	$N = 64$	$N = 128$	$m = 64$	$m = 128$
0	0	0	0	0	0	0.000203	0
0.1	0.005	0.00499998	0.005	0.0049789	0.0499965	0.00157	0.004587
0.2	0.020	0.0199999	0.020	0.0199693	0.0199989	0.021056	0.02054
0.3	0.045	0.0449998	0.045	0.0449485	0.0449988	0.040154	0.04328
0.4	0.080	0.0799996	0.080	0.0799275	0.0799980	0.086581	0.081564
0.5	0.125	0.124999	0.125	0.1249110	0.1249941	0.12058	0.126196
0.6	0.180	0.179999	0.180	0.1799068	0.1799840	0.17985	0.18346
0.7	0.245	0.244999	0.245	0.2448798	0.2449730	0.23982	0.247982
0.8	0.320	0.319999	0.320	0.3198459	0.3199785	0.323195	0.32120
0.9	0.405	0.404998	0.405	0.4046765	0.4049762	0.03905	0.406365
Max error	0	1.692071e−6	5.786662e−8	1.97e−4	3.21e−5	7.23e−3	2.88e−3

tested on an Intel(R) Core(TM) i5-2450M CPU @ 2.50GHz Processor with 4 GB of RAM using Maple 2018 software on Windows 7 (64 bit) operating system with 16 significant digits (Digits:= 16). The absolute errors in the solutions are obtained by

$$\left|f(x, y) - f_{N,M}(x, y)\right|, \qquad (x, y) \in [0, \ell_1) \times [0, \ell_2), \ N, M \in \mathbb{N}.$$

Also, the maximum absolute errors

$$\max_{i,j=1,\ldots,NM} \left\{\left|f(x_i, y_j) - f_{N,M}(x_i, y_j)\right|\right\},$$

are calculated at points $(x_i, y_j),\ i, j = 1, \ldots, NM$ which are Newton-Cotes nodes in $[0, \ell_1) \times [0, \ell_2)$.

Moreover, plots of maximum absolute errors are displayed by using

$$\max_{j=1,\ldots,NM} \left\{\left|f(x, y_j) - f_{N,M}(x, y_j)\right|\right\}, \qquad x \in [0, \ell_1),$$

where points $y_j,\ j = 1, \ldots, NM$ are Newton-Cotes nodes in $[0, \ell_2)$.

Example 1 Consider the following two-dimensional fractional Fredholm integral equation studied by Hesameddini and Shahbazi (2018); Najafalizadeh and Ezzati (2016):

$$f(x, y) = \frac{2362}{4725}xy + \frac{1}{\Gamma(\frac{7}{2})\Gamma(\frac{7}{2})} \int_0^1 \int_0^1 (1-\tau)^{\frac{5}{2}}(1-\varsigma)^{\frac{5}{2}} xy\sqrt{\varsigma}\, f(\tau, \varsigma) \mathrm{d}\varsigma \mathrm{d}\tau,$$

with the exact solution $f(x, y) = \frac{1}{2}xy$.

In Tables 1 and 2, respectively, we report the exact and approximate solutions and also the absolute errors in the solutions for $N = 2,\ M = 2, 3$ at some selected nodes. These tables state that by using $\hat{n} = N^2M^2 = 36$ numbers of bases, we obtain more accurate results than the 2D-SLPOM and 2D-BPFs methods reported by Hesameddini and Shahbazi (2018); Najafalizadeh and Ezzati (2016), respectively, that used $\hat{n} = (N+1)^2 = 129^2 = 16641$ 2D-SLPOM and $\hat{n} = m^2 = 128^2 = 16384$ 2D-BPFs to solve this problem. Figures 1 and 2 illustrate the accuracy and efficiency of the presented method.

Table 2 Absolute errors for Example 1

$x = y$	Present method		2D-BPFs	
	$M = 2$	$M = 3$	$m = 16$	$m = 32$
0	0	5.000000e−17	1.14e−3	6.14e−4
0.1	2.210053e − 8	6.886606e−10	1.67e−2	6.24e−3
0.2	8.840210e−8	2.754642e−9	1.09e−2	7.93e−3
0.3	1.989047e−7	6.197945e−9	1.62e−2	7.22e−3
0.4	3.536084e−7	1.101857e−8	9.23e−3	2.53e−3
0.5	5.525131e−7	1.721651e−8	2.58e−2	1.32e−2
0.6	7.956189e−7	2.479178e−8	7.44e−3	4.61e−3
0.7	1.082926e−6	3.374437e−8	2.58e−2	1.48e−2
0.8	1.414434e−6	4.407428e−8	9.97e−3	5.27e−3
0.9	1.790143e−6	5.578151e−8	2.32e−2	1.32e−2

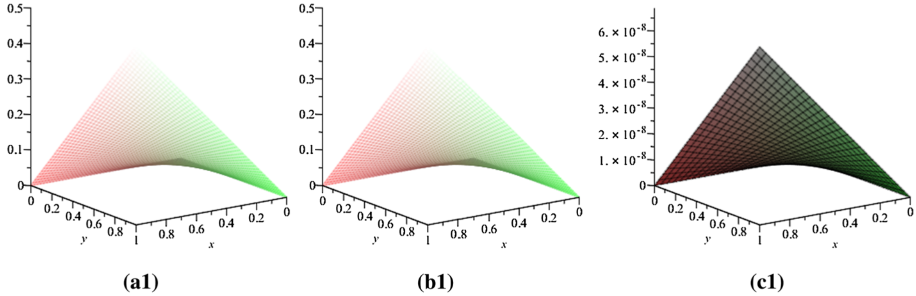

Fig. 1 Plots of: **a1** the exact solution, **b1** the approximate solution, **c1** the absolute error with $N = 2$ and $M = 3$ for Example 1

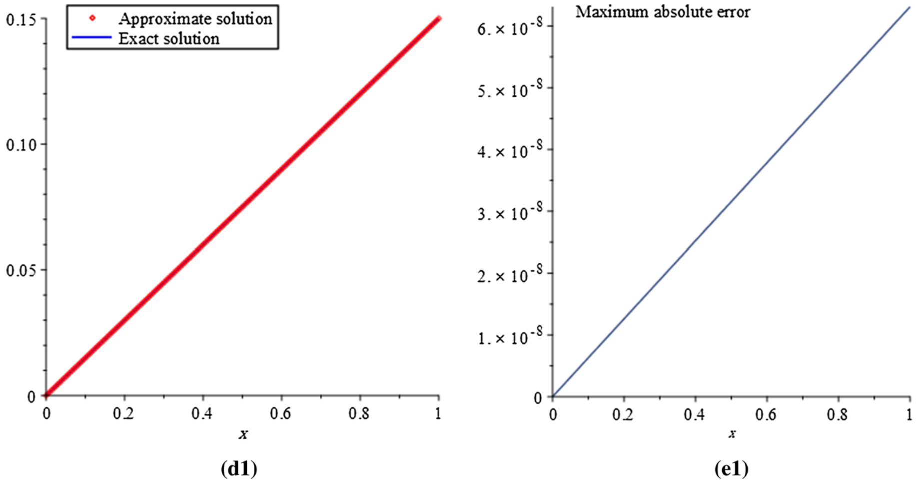

Fig. 2 Plots of: **d1** the comparison of the exact and approximate solutions, **e1** the maximum absolute error with $N = 2$ and $M = 3$ at $y = 0.3$ for Example 1

Table 3 Numerical results for Example 2

$x = y$	Exact solution	Present method		2D-SLPM		2D-BPFs	
		$M = 2$	$M = 3$	$N = 64$	$N = 128$	$m = 64$	$m = 128$
0	0	−0.0416667	−6.87500e − 17	0.0001429	0.0000062	0.000203	0
0.1	−0.04	−0.0416667	−0.04	−0.0399150	−0.0399967	0.00157	0.004587
0.2	−0.06	−0.0416667	−0.06	−0.0599359	−0.0599927	0.021056	0.02054
0.3	−0.06	−0.0416667	−0.06	−0.0598965	−0.0599967	0.040154	0.04328
0.4	−0.04	−0.0416667	−0.04	−0.0398165	−0.0399968	0.086581	0.081564
0.5	0	−0.0416667	−1.50625e − 16	0.0002158	0.0000014	0.12058	0.126196
0.6	0.06	0.0583333	0.06	0.0597465	0.0599936	0.17985	0.18346
0.7	0.14	0.158333	0.14	0.1396887	0.1399886	0.23982	0.247982
0.8	0.24	0.258333	0.24	0.2396555	0.2399852	0.323195	0.32120
0.9	0.36	0.358333	0.36	0.3598051	0.3599875	0.03905	0.406365
Max error	0	5.234025e−3	1.096591e−5	1.97e−4	3.21e−5	7.23e−3	2.88e−3

Table 4 Absolute errors for Example 2

$x = y$	Present method		2D-BPFs	
	$M = 2$	$M = 3$	$m = 16$	$m = 32$
0	4.166667e−2	6.875000e−17	2.95e−2	1.42e−2
0.1	1.666667e−3	0	4.05e−2	2.13e−2
0.2	1.833333e−2	1.000000e − 17	4.94e−2	1.96e−2
0.3	1.833333e−2	0	4.94e−2	1.96e−2
0.4	1.666667e−3	0	4.05e−2	2.13e−2
0.5	4.166667e−2	1.506250e−16	2.95e−2	1.42e−2
0.6	1.666667e−3	8.000000e−17	4.94e−2	1.39e−1
0.7	1.833333e−2	0	4.10e−2	2.06e−2
0.8	1.833333e−2	0	2.10e−2	5.86e−3
0.9	1.666667e−3	1.000000e − 16	4.12e−2	2.06e−2

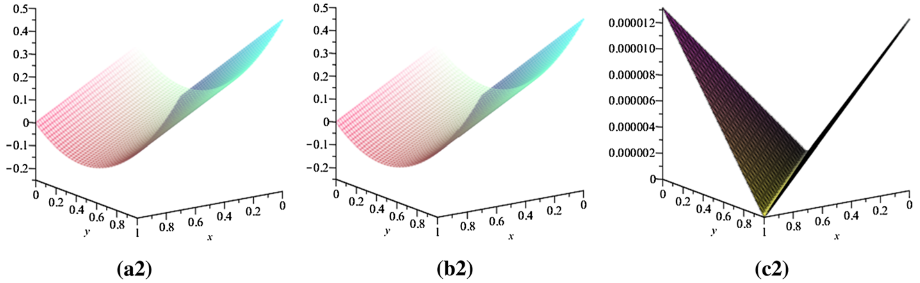

Fig. 3 Plots of: **a2** the exact solution, **b2** the approximate solution, **c2** the absolute error with $N = 2$ and $M = 3$ for Example 2

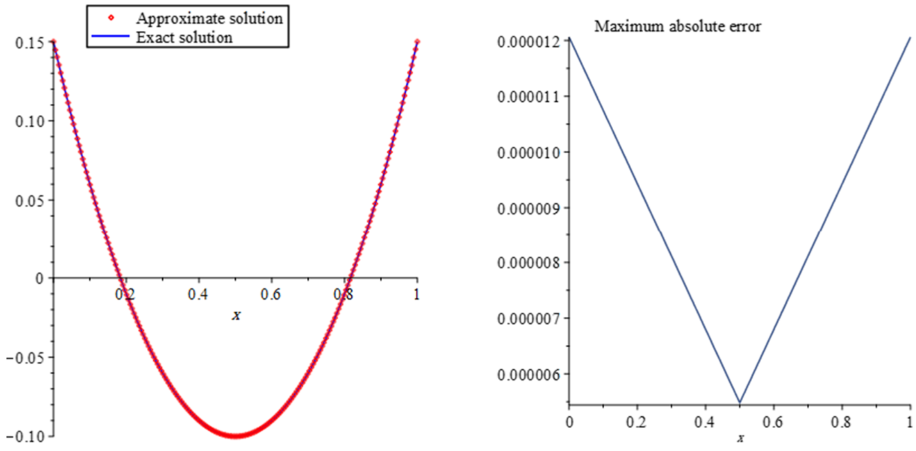

(d2) **(e2)**

Fig. 4 Plots of: **d2** the comparison of the exact and approximate solutions, **e2** the maximum absolute error with $N = 2$ and $M = 3$ at $y = 0.3$ for Example 2

Table 5 Numerical results for Example 3

$x = y$	Exact solution	Present method		2D-BPFs	
		$M = 3$	$M = 4$	$m = 16$	$m = 32$
0	0	0.00848361	0.00465488	0.018452	0.009386
0.1	0.057735	0.0516175	0.0555976	0.031135	0.042121
0.2	0.115470	0.114056	0.118617	0.132610	0.124282
0.3	0.173205	0.179512	0.17389	0.147605	0.156905
0.4	0.230940	0.235315	0.227048	0.246768	0.239179
0.5	0.288675	0.289481	0.288775	0.262075	0.274574
0.6	0.346410	0.346123	0.34638	0.360925	0.354075
0.7	0.404145	0.403988	0.404194	0.378545	0.389848
0.8	0.461880	0.462224	0.461945	0.475083	0.468971
0.9	0.519615	0.52003	0.519653	0.501015	0.507021
Max error	0	9.395571e−3	6.527875e−3	2.96e−2	1.63e−2

Example 2 Consider the following two-dimensional fractional Fredholm integral equation studied by Hesameddini and Shahbazi (2018) and Najafalizadeh and Ezzati (2016):

$$f(x, y) = g(x, y) + \frac{1}{\Gamma(\frac{9}{2})\Gamma(\frac{3}{2})} \int_0^1 \int_0^1 (1-\tau)^{\frac{7}{2}} (1-\varsigma)^{\frac{1}{2}} 5\sqrt{\tau}(y-x) f^2(\tau, \varsigma) \mathrm{d}\varsigma \mathrm{d}\tau,$$

where

$$g(x, y) = \frac{322560x^2 - 322349x + 161069y}{322560},$$

with the exact solution $f(x, y) = x^2 - x + \frac{1}{2}y$.

Table 6 Absolute errors for Example 3

$x = y$	Present method		2D-TFs method		2D-BPFs method	
	$M = 3$	$M = 4$	$m = 6$	$m = 8$	$m = 16$	$m = 32$
0	8.483608e−3	4.654879e−3	0	0	1.84e−2	9.38e−3
0.1	6.117569e−3	2.137467e−3	0.020069	0.008448	2.66e−2	1.56e−2
0.2	1.413861e−3	3.146985e−3	0.00764	0.002634	1.71e−2	8.81e−3
0.3	6.306532e−3	6.853207e−4	0.000789	0.005404	2.56e−2	1.63e−2
0.4	4.375111e−3	3.891639e−3	0.003448	0.000709	1.57e−2	8.23e−3
0.5	8.055251e−4	1.002373e−4	0.006956	0.007308	2.66e−2	1.41e−2
0.6	2.875908e−4	3.036785e−5	0.000093	0.000053	1.45e−2	7.66e−3
0.7	1.571449e−4	4.901139e−5	0.000335	0.000044	2.56e−2	1.42e−2
0.8	3.433532e−4	6.500334e−5	0.001909	0.001421	1.32e−2	7.09e−3
0.9	4.150370e−4	3.739562e−5	0.003807	0.003041	1.86e−2	1.25e−2

In Tables 3 and 4, respectively, we report the exact and approximate solutions and also the absolute errors in the solutions for $N = 2,\ M = 2, 3$ at some selected nodes. These tables state that using $\hat{n} = N^2M^2 = 36$ numbers of bases, we obtain more accurate results than the 2D-SLPOM and 2D-BPFs methods reported by Hesameddini and Shahbazi (2018); Najafalizadeh and Ezzati (2016), respectively, that used $\hat{n} = (N + 1)^2 = 129^2 = 16641$ 2D-SLPOM and $\hat{n} = m^2 = 128^2 = 16384$ 2D-BPFs to solve this problem. Figures 3 and 4 illustrate the accuracy and efficiency of the presented method.

Example 3 Consider the following two-dimensional nonlinear fractional Volterra integral equation studied by Jabari Sabeg et al. (2017) and Najafalizadeh and Ezzati (2016):

$$f(x, y) = \sqrt{y}\left(-\frac{1}{180}x^3 y^{\frac{7}{2}} + \sqrt{\frac{x}{3}}\right) + \frac{1}{\Gamma\left(\frac{3}{2}\right)\Gamma\left(\frac{5}{2}\right)}\int_0^x \int_0^y (x-\tau)^{\frac{1}{2}}(y-\varsigma)^{\frac{3}{2}}\sqrt{xy\varsigma}\, f^2(\tau, \varsigma)\mathrm{d}\varsigma\mathrm{d}\tau,$$

with the exact solution $f(x, y) = \frac{\sqrt{3xy}}{3}$.

The exact and approximate solutions and also the absolute errors in the solutions, respectively, are reported in Tables 5 and 6 for $N = 2,\ M = 3, 4$. These tables state that by using $\hat{n} = N^2M^2 = 64$ numbers of bases, we obtain more accurate results than the 2D-TFs and 2D-BPFs methods reported by Jabari Sabeg et al. (2017) and Najafalizadeh and Ezzati (2016), respectively, that used $\hat{n} = 4m^2 = 256$ 2D-TFs and $\hat{n} = m^2 = 32^2 = 1024$ 2D-BPFs to solve this problem. Figures 5 and 6 illustrate the accuracy and efficiency of the presented method.

8 Conclusion

In the presented paper, sufficient conditions were provided for the local and global existence of solutions for 2D-NFVIEs and 2D-NFFIEs, based on the Schauder's and Tychonoff's fixed-point theorems. Also, sufficient conditions were provided for the uniqueness of the solutions.

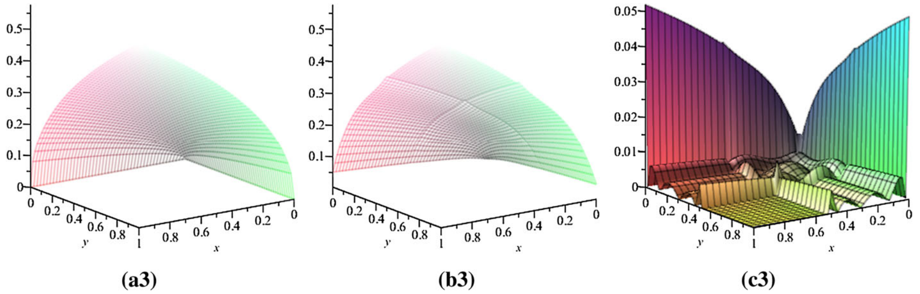

Fig. 5 Plots of: **a3** the exact solution, **b3** the approximate solution, **c3** the absolute error with $N = 2$ and $M = 4$ for Example 3

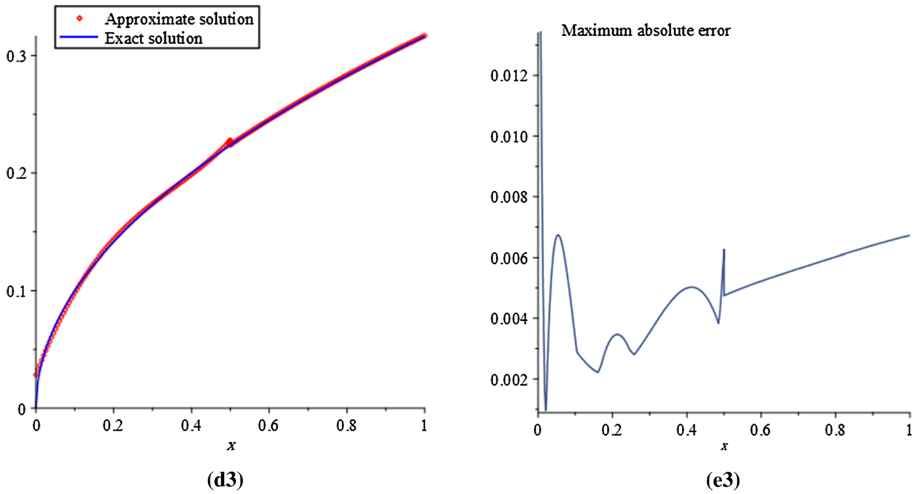

Fig. 6 Plots of: **d3** the comparison of the exact and approximate solutions, **e3** the maximum absolute error with $N = 2$ and $M = 4$ at $y = 0.3$ for Example 3

Moreover, operational matrices of 2D-HBPSLs via collocation method were applied to find approximate solutions for 2D-NFVIEs and 2D-NFFIEs. The obtained results introduced the presented method as a powerful mathematical tool for solving these fractional integral equations with lower numbers of bases than the other methods studied by Hesameddini and Shahbazi (2018); Jabari Sabeg et al. (2017); Najafalizadeh and Ezzati (2016).

Acknowledgements The authors express their sincere thanks to the reviewer for his valuable comments and suggestions that improved the content of the paper.

References

Abbas S, Benchohra M (2014) Fractional order integral equations of two independent variables. Appl Math Comput 227:755–761

Ahmed E, Elgazzar AS (2007) On fractional order differential equations model for nonlocal epidemics. Phys A 379(2):607–614

Amin R, Shah K, Asif M, Khan I, Ullah F (2021) An efficient algorithm for numerical solution of fractional integro-differential equations via Haar wavelet. J Comput Appl Math 381:113028
Aminikhah H, Sheikhani AHR, Houlari T, Rezazadeh H (2017) Numerical solution of the distributed-order fractional Bagley–Torvik equation. J Autom Sin epub 6(3):760–765
Atanackovic TM, Stankovic B (2004) On a system of differential equations with fractional derivatives arising in rod theory. J Phys A: Math Gen 37(4):1241
Chen W (2006) A speculative study of 2/3-order fractional Laplacian modeling of turbulence: some thoughts and conjectures. Chaos 16(2): Article ID 023126
Chen W, Sun H, Zhang X, Korosak D (2010) Anomalous diffusion modeling by fractal and fractional derivatives. Comput Math Appl 59(5):1754–1758
Cheney EW (1966) Introduction to approximation theory. McGraw-Hill, New York
Conway JB (2007) A course in functional analysis. Springer, Berlin
Dahaghin MS, Hassani H (2017) An optimization method based on the generalized polynomials for nonlinear variable-order time fractional diffusion-wave equation. Nonlinear Dyn 88(3):1587–1598
Davis P (1975) Interpolation and approximation. Blaisdell, New York
Esmaeili SH, Shamsi M, Luchkob Y (2011) Numerical solution of fractional differential equations with a collocation method based on Müntz polynomials. Comput Math Appl 62:918–929
Evans RM, Katugampola UN, Edwards DA (2017) Applications of fractional calculus in solving Abel-type integral equations: surface-volume reaction problem. Comput Math Appl 73(6):1346–1362
Fathizadeh E, Ezzati R, Maleknejad K (2017) The construction of operational matrix of fractional integration using the fractional chebyshev polynomials. Int J Appl Comput Math 3(1):387–409
Hassani H, Avazzadeh Z, Tenreiro Machado JA (2019) Numerical approach for solving variable-order space-time fractional telegraph equation using transcendental Bernstein series. Eng Comput. https://doi.org/10.1007/s00366-019-00736-x
Hassani H, Naraghirad E (2019) A new computational method based on optimization scheme for solving variable-order time fractional Burgers' equation. Math Comput Simul 162:1–17
Hassani H, Tenreiro Machado JA, Avazzadeh Z (2019a) An effective numerical method for solving nonlinear variable-order fractional functional boundary value problems through optimization technique. Nonlinear Dyn 97(4):2041–2054
Hassani H, Tenreiro Machado JA, Naraghirad E (2019b) Generalized shifted Chebyshev polynomials for fractional optimal control problems. Commun Nonlinear Sci Numer Simul 75:50–61
Hesameddini E, Shahbazi M (2018) Two-dimensional shifted Legendre polynomials operational matrix method for solving the two-dimensional integral equations of fractional order. Appl Math Comput 322:40–54
Jabari Sabeg D, Ezzati R, Maleknejad K (2017) A new operational matrix for solving two-dimensional nonlinear integral equations of fractional order. Cogent Math 4(1):1347017. https://doi.org/10.1080/23311835.2017.1347017
Kılıçman A, Al Zhour ZAA (2007) Kronecker operational matrices for fractional calculus and some applications. Appl Math Comput 187(1):250–265
Kreyszig E (1989) Introductory functional analysis with applications. Wiley, New York
Li Y, Shah K (2017) Numerical solutions of coupled systems of fractional order partial differential equations. Adv Math Phys. Article ID 1535826:1–14
Maleknejad K, Rashidinia J, Eftekhari T (2018) Numerical solution of three-dimensional Volterra–Fredholm integral equations of the first and second kinds based on Bernstein's approximation. Appl Math Comput 339:272–285
Maleknejad K, Rashidinia J, Eftekhari T (2020a) Operational matrices based on hybrid functions for solving general nonlinear two-dimensional fractional integro-differential equations. Comp Appl Math 39:103. https://doi.org/10.1007/s40314-020-1126-8
Maleknejad K, Rashidinia J, Eftekhari T (2020b) Numerical solutions of distributed order fractional differential equations in the time domain using the Müntz-Legendre wavelets approach. Numer Methods Partial Differ Equ. https://doi.org/10.1002/num.22548
Maleknejad K, Rashidinia J, Eftekhari T (2020c) A new and efficient numerical method based on shifted fractional-order Jacobi operational matrices for solving some classes of two-dimensional nonlinear fractional integral equations. Submitted to Numerical Methods for Partial Differential Equations
Mashoof M, Refahi Shekhani AH (2017) Simulating the solution of the distributed order fractional differential equations by block-pulse wavelets. UPB Sci Bull Ser A Appl Math Phys 79:193–206
Mirzaee F, Samadyar N (2019) Numerical solution based on two-dimensional orthonormal Bernstein polynomials for solving some classes of two-dimensional nonlinear integral equations of fractional order. Appl Math Comput 344–345:191–203
Mohammadi Rick S, Rashidinia J (2019) Solving fractional diffusion equations by Sinc and radial basis functions. Asian-Eur J Math 2050101. https://doi.org/10.1142/S1793557120501016

Najafalizadeh S, Ezzati R (2016) Numerical methods for solving two-dimensional nonlinear integral equations of fractional order by using two-dimensional block pulse operational matrix. Appl Math Comput 280:46–56

Nouri K, Torkzadeh L, Mohammadian S (2018) Hybrid Legendre functions to solve differential equations with fractional derivatives. Math Sci 12:129–136

Permoon MR, Rashidinia J, Parsa A, Haddadpour H, Salehi R (2016) Application of radial basis functions and sinc method for solving the forced vibration of fractional viscoelastic beam. J Mech Sci Technol 30(7):3001–3008

Podlubony I (1999) Fract Diff Equ. Academic Press, San Diego

Pourbabaee M, Saadatmandi A (2019) A novel Legendre operational matrix for distributed order fractional differential equations. Appl Math Comput 361:215–231

Rahimkhani P, Ordokhani Y, Babolian E (2018) M*ü*ntz-Legendre wavelet operational matrix of fractional-order integration and its applications for solving the fractional pantograph differential equations. Numer Algor 77:1283–1305

Rossikhin YA, Shitikova MV (1997) Application of fractional derivatives to the analysis of damped vibrations of viscoelastic single mass systems. Acta Mech 120(1):109–125

Saeedi H, Mohseni Moghadam M (2011) Numerical solution of nonlinear Volterra integro-differential equations of arbitrary order by CAS wavelets. Commun Nonlinear Sci Numer Simul 16:1216–1226

Samadyar N, Mirzaee F (2019) Numerical scheme for solving singular fractional partial integro-differential equation via orthonormal Bernoulli polynomials. Int J Num Model 32(6):e2652

Shah K, Wang J (2019) A numerical scheme based on non-discretization of data for boundary value problems of fractional order differential equations. RACSAM 113:2277–2294

Sun HG, Chen W, Chen YQ (2009) Variable-order fractional differential operators in anomalous diffusion modeling. Phys A 388(21):4586–4592

Sun HG, Chen D, Zhang Y, Chen L (2015) Understanding partial bed-load transport: experiments and stochastic model analysis. J Hydrol 521:196–204

Zalp N, Demirci E (2011) A fractional order SEIR model with vertical transmission. Math Comput Model 54(1–2):1–6

Zeidler E (1995) Applied functional analysis: applications to mathematical physics. Appl Math Sci 108

Zhu L, Fan Q (2012) Solving fractional nonlinear Fredholm integro-differential equations by the second kind Chebyshev wavelet. Commun Nonlinear Sci Numer Simul 17:2333–2341